

Probing the charge-transfer state of CO on Pt(111) by two-dimensional infrared-visible sum frequency generation spectroscopy

K. C. Chou,^{1,3,*} S. Westerberg,^{1,3} Y. R. Shen,^{2,3} P. N. Ross,³ and G. A. Somorjai^{1,3,†}

¹Department of Chemistry, University of California, Berkeley, California 94720, USA

²Department of Physics, University of California, Berkeley, California 94720, USA

³Materials Science Division, Lawrence Berkeley National Laboratory, Berkeley, California 94720, USA

(Received 25 November 2003; revised manuscript received 20 January 2004; published 30 April 2004)

The lowest charge-transfer band of CO on Pt(111) was identified using two-dimensional infrared-visible sum frequency generation spectroscopy. The electronic resonance associated with the stretching mode of atop CO appeared at 2.51 eV with a bandwidth of 0.83 eV. The result is consistent with earlier calculations using CO-Pt cluster models indicating that the resonance is from $5d$ to $6sp$ orbital of Pt hybridized with orbital of CO. The measured transition energy suggests that the antibonding state of Pt $6sp$ and CO 5σ for atop CO on Pt(111) is ~ 2.2 eV above Fermi level.

DOI: 10.1103/PhysRevB.69.153413

PACS number(s): 73.20.-r, 39.30.+w, 42.65.-k, 82.65.+r

Infrared-visible sum frequency generation (SFG) spectroscopy has been proven to be a powerful tool for a broad range of interfacial studies on physical, chemical, and biological systems.^{1,2} In most cases, it has been used as a one-dimensional vibrational spectroscopy by tuning the IR frequency over vibrational transitions at the interfaces. However, it is possible to have both IR and visible frequencies tunable, allowing two-dimensional (2D) spectroscopic probing of vibrational and electronic transitions of a surface simultaneously.³ Aside from enhanced signals due to double resonance, this scheme has the advantage of having a better selectivity in identifying the electronic transitions at a surface. In this paper, we applied the technique to locate surface electronic states induced by molecular adsorbates at a metal surface. Such states are important for understanding surface processes such as electron and energy transfer, catalytic reactions,⁴ photoinduced reactions,⁵ and surface-enhanced spectroscopy.⁶ In 2D SFG, the intensity enhancement of an adsorbate vibrational mode, as the visible frequency approaches a surface electronic transition, indicates that the excited electronic state must be effectively coupled to the adsorbates. In comparison to other techniques, such as photoemission spectroscopy (PES)⁷ and second-harmonic generation,¹ 2D SFG has a number of advantages. First, it is more species specific because of the vibrational resonance. It avoids uncertainty in peak assignment, especially when more than one kind of adsorbates (or different functional groups on larger molecules) are present at the interface. Second, it is more surface specific because the observed electronic transition must be vibronically coupled with the adsorbate. It avoids interference from the bulk signals. In addition, unlike PES, 2D SFG can also be applied to surfaces under ambient conditions and to any interfaces accessible by probing beams.

To demonstrate that 2D SFG is an effective technique to probe adsorbate-induced surface states, we chose CO on Pt(111) as a representative case because CO/Pt(111) is one of the most studied model systems in surface science.⁸ For free CO, the lowest electronic excitation is in the UV region. Upon adsorption on Pt(111), the unoccupied $2\pi_a^*$ state has

been identified to be at 4.3 eV above the Fermi level by inverse photoemission⁹ and two-photon photoemission¹⁰ (see Fig. 1). However, the lowest unoccupied electronic state $5\sigma_a$ has never been detected despite its importance for understanding surface charge-transfer⁴, photo induced processes⁵ and surface-enhanced Raman scattering (SERS).⁶ SERS has been widely used to investigate the vibrational properties of adsorbed molecules. While the electromagnetic enhancement on roughened metallic surfaces may be the dominating factor for SERS, the chemical enhancement mechanism has always been suggested as a possible mechanism contributing to SERS.¹¹ However, it has been difficult to study the chemical enhancement mechanism because a direct measurement of the adsorbate-induced surface states has been absent. Here, we present the first spectroscopic observation of electronic transition to a charge-transfer band on a flat metal surface using 2D SFG. We found a surface electronic resonance at 2.51 eV for CO/Pt(111) that vibronically coupled with the stretching mode of the adsorbed CO. The observed energy level is consistent with the theoretical calculations of Nakatsuji *et al.*¹² and Wu *et al.*¹³ SERS on flat metal surface has been difficult due to low intensity. Our ability to carry out the experiment on a flat single-crystal surface allows us to ex-

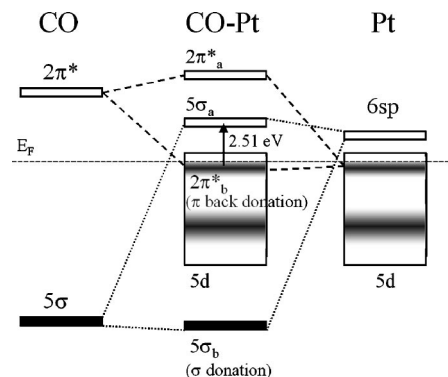


FIG. 1. A schematic orbital diagram for the interaction between CO and Pt. (Black indicates occupied states and white indicates vacant states.) The arrow describes the measured electronic transition.

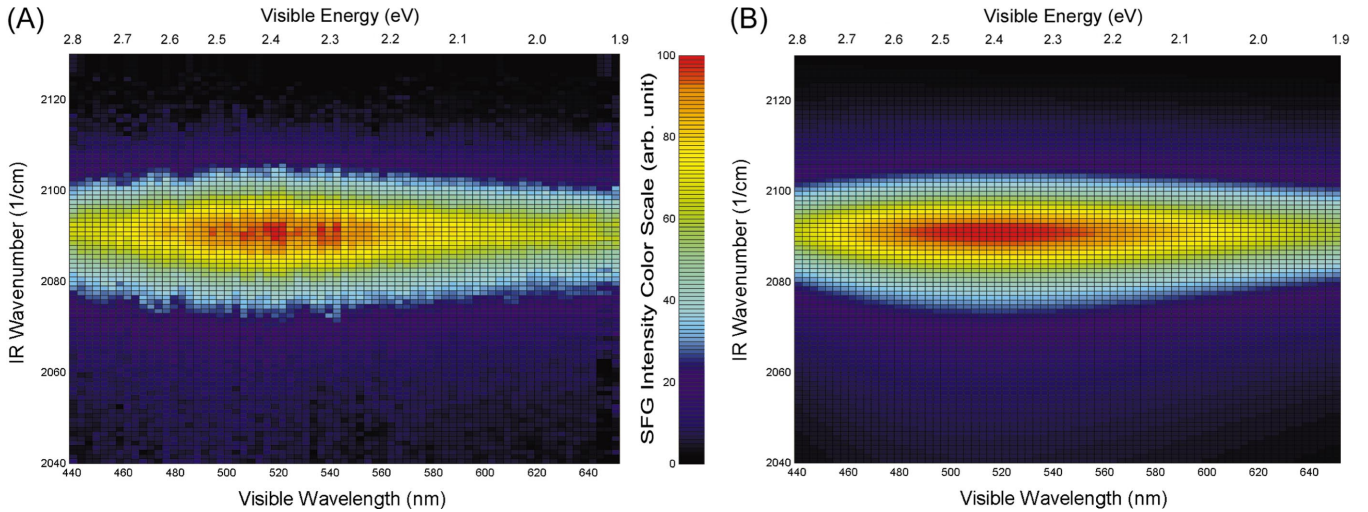


FIG. 2. (Color) (a) Measured SFG intensity for CO on Pt(111) as a function of IR and visible frequencies. A double-resonance peak is seen as indicated by red color. (b) The fitting curve of the measured two-dimensional SFG spectra using Eq. (1), (4), and (6).

clude the electromagnetic enhancement mechanism and provides a direct experimental evidence for the chemical enhancement to surface-enhanced spectroscopy.

Our experiments were carried out with the sample under UHV conditions (1×10^{-10} Torr). The Pt(111) surface was prepared by cycles of argon ion sputtering at room temperature and thermal annealing at 850°C until a sharp (1×1) low-energy electron-diffraction pattern was observed. To obtain a saturation coverage, CO was dosed at 1×10^{-6} Torr for 10 sec. Optical measurements were performed using a Nd:YAG(yttrium aluminum garnet) laser at 1064 nm with 20 ps pulse width and 20 Hz repetition rate. The laser was used to generate harmonics at 532 and 355 nm in KTP crystals to pump two optical parametric generators/amplifiers (OPG/OPA). The tunable IR beam was produced by difference frequency mixing of the 1064 nm beam with the output of a KTP OPG/OPA pumped by the 532 nm beam. The tunable visible beam was generated by a BBO-OPG/OPA pumped by the 355 nm beam. The spectral bandwidths of the visible and IR beams were about 7 cm^{-1} . The visible and IR beams were overlapped both spatially and temporally on the sample at incident angles of 60° and 50° , respectively. The IR beam was focused on the sample and had a spot size of 3.2 mm full width at half maximum. To improve the mode quality of the visible beam and avoid beam walk during wavelength tuning, a flat top visible beam was imaged onto the sample with a diameter of 3 mm.

The fluence of the visible beam was 0.2 mJ/cm^2 per pulse, which was an order of magnitude smaller than that in a typical photodesorption experiment. No photoinduced desorption of CO was observed during our experiment. The SFG intensity was detected by a photomultiplier tube (Hamamatsu R3896) after spectral filtering by a color filter and a double monochromator. The measured SFG intensity was calibrated by the wavelength dependence of the sensitivity of the photomultiplier and the throughput of the color filter and monochromator. Since SFG from the bridged CO on Pt(111) suffers greatly from low sensitivity at room temperature,¹⁴ we focused our study on the atop CO that has

a stretching mode at 2090 cm^{-1} . The IR wave number was scanned from 2040 to 2130 cm^{-1} in 1 cm^{-1} steps for each visible frequency. Then the visible frequency was changed from 439 to 652 nm with a step of 3 nm. For each SFG spectral scan, the energies of the visible and IR beams were kept at 20 and $70\ \mu\text{J}$ per pulse, respectively. All spectra were taken using PPP polarization combination (P polarized for SFG, visible, and IR beams). Each data point is an average of 60 laser shots.

Figure 2(a) describes the measured SFG output as a function of IR and visible frequencies. A doubly resonant peak shown by the red color is clearly seen with the IR resonance around 2090 cm^{-1} and the visible resonance between 2.2 eV and 2.6 eV. The IR resonance around 2090 cm^{-1} is the stretching frequency for CO at atop sites. This doubly resonant feature assures that the observed electronic resonance arises from the electronic states of the atop CO/Pt(111) chemisorption system.

The SFG output intensity (in SI units) at frequency $\omega_s = \omega_1 + \omega_2$ in the reflected direction is given by¹

$$I(\omega_s) = \frac{\omega_s^2}{8\epsilon_0 c^3 \cos^2 \beta_s} |\chi_{eff}^{(2)}|^2 I(\omega_1) I(\omega_2), \quad (1)$$

with

$$\chi_{eff}^{(2)} = [\mathbf{L}(\omega_s) \cdot \mathbf{e}_s] : \chi^{(2)} : [\mathbf{L}(\omega_1) \cdot \mathbf{e}_1][\mathbf{L}(\omega_2) \cdot \mathbf{e}_2], \quad (2)$$

where β_s , $I(\omega_i)$, $\mathbf{L}(\omega_i)$, and \mathbf{e}_i are the reflected SFG angle, input intensity, tensorial Fresnel factor, and the unit polarization vector of the field at frequency ω_i , respectively. The second-order nonlinear susceptibility $\chi^{(2)}$ is related to the molecular hyperpolarizability $\alpha^{(2)}$ by

$$\chi_{ijk}^{(2)} = N_s \sum_{a,b,c} \langle (\hat{i} \cdot \hat{a})(\hat{j} \cdot \hat{b})(\hat{k} \cdot \hat{c}) \rangle \alpha_{abc}^{(2)}, \quad (3)$$

where N_s is the surface density of molecules, and $\hat{i}\hat{j}\hat{k}$ and $\hat{a}\hat{b}\hat{c}$ describe the lab and molecular coordinates, respectively.

For CO with a cylindrical symmetry, only $\alpha_{aac}^{(2)} = \alpha_{bbc}^{(2)}$ and $\alpha_{ccc}^{(2)}$ with c axis along the bond axis are nonvanishing. Surface isotropy about the surface normal along the z axis allows only $\chi_{xxz}^{(2)} = \chi_{yyz}^{(2)}$, $\chi_{xzx}^{(2)} = \chi_{yzy}^{(2)} = \chi_{zxx}^{(2)} = \chi_{zyy}^{(2)}$, and $\chi_{zzz}^{(2)}$ to be nonzero. For metal surfaces, the Fresnel coefficients greatly reduce the S -polarized field components and make the contributions of all $\chi_{ijk}^{(2)}$ negligible except $\chi_{zzz}^{(2)}$. Consequently, SFG with PPP polarization should dominate.

$$\chi_{eff,PPP}^{(2)} \approx L_{zz}(\omega_s) L_{zz}(\omega_1) L_{zz}(\omega_2) \sin \beta_s \sin \beta_1 \sin \beta_2 \chi_{zzz}^{(2)}, \quad (4)$$

with

$$L_{zz}(\omega_i) = \frac{2n(\omega_i) \cos \beta_i}{\cos \gamma_i + n(\omega_i) \cos \beta_i}, \quad (5)$$

where β_i , γ_i , and $n(\omega_i)$ are the incident angle, the refracted angle, and the refraction index of Pt at frequency ω_i ,¹⁵ respectively. Experimentally, we obtained $I_{SSP}/I_{PPP} < 5 \times 10^{-3}$. Our inability to measure I_{SSP}/I_{PPP} prevents us from determining the average orientation of CO on Pt(111), but previous angle-resolved photoemission study shows that CO is oriented perpendicular to the surface.¹⁶

There are two types of processes that contribute to SFG: one begins with an electronic transition followed by a vibrational transition (Vis-IR), and the other begins with a vibrational transition followed by an electronic transition (IR-Vis). Because of the significantly broader bandwidths of electronic and vibronic resonances, the contribution of the Vis-IR SFG is much smaller than that of the IR-Vis SFG.¹⁷ Taking into account only the IR-Vis processes, the doubly resonant $\alpha^{(2)}$ or $\chi_{zzz}^{(2)}$ in our case has the dispersion:

$$\chi_{zzz}^{(2)} \propto \frac{1}{\omega_{IR} - \omega_0 + i\Gamma_0} \left\{ \frac{1}{\omega_{IR} + \omega_{vis} - \omega_e + i\Gamma_e} - \frac{1-S}{\omega_{IR} + \omega_{vis} - \omega_0 - \omega_e + i\Gamma'_e} \right\}, \quad (6)$$

where ω_0 and ω_e are the CO stretching frequency and electronic resonant frequency, respectively. S is the vibronic coupling constant (Huang-Rhys factor), and Γ 's are the damping constants. Here, we have neglected multivibrational excitations. Equation (6) consists of two peaks which are separated from each other in energy by the vibrational energy of CO. The first term in Eq. (6) shows a resonant enhancement when $\omega_{IR} + \omega_{vis} \approx \omega_e$ and the second term has a resonance when $\omega_{IR} + \omega_{vis} \approx \omega_0 + \omega_e$.

Figure 2(b) shows the two-dimensional fitting of the measured spectrum in Fig. 2(a) using Eqs. (1), (4), and (6) with ω_0 , Γ_0 , ω_e , $\Gamma_e = \Gamma'_e$, S , and an additional nonresonant susceptibility $\chi_{NR}^{(2)}$ as fitting parameters. The best fit was obtained with $\omega_0 = 2091.1 \pm 0.3 \text{ cm}^{-1}$, $\Gamma_0 = 9.0 \pm 0.3 \text{ cm}^{-1}$, $\omega_e = 2.51 \pm 0.01 \text{ eV}$, $\Gamma_e = \Gamma'_e = 0.83 \pm 0.01 \text{ eV}$, and $S < 1 \times 10^{-6}$. Due to the broad width of the electronic resonance and a relatively small vibrational energy of CO, the vibronic sideband is not clearly resolved in our measurements. The vibrational mode at 2091 cm^{-1} comes from the stretching

mode of CO adsorbed at the atop sites of Pt(111).¹⁸ The electronic resonance at 2.51 eV falls in the range of the $5d$ to $6sp$ transition of Pt under the perturbation of the chemisorbed CO as predicted by Nakatsuji *et al.*¹² It is also in good agreement with the CO-Pt₈ cluster calculation of Wu *et al.* that shows four possible Raman transitions at 1.66, 2.15, 2.41, and 2.58 eV with the intensity of the 2.58 eV transition an order of magnitude larger than the others.¹³ The observed SFG spectra indicate that the electronic resonance is vibronically coupled to the CO stretching mode and therefore belongs to the CO/Pt chemisorption system.

The adsorption of CO on Pt is often described by the Blyholder model as sketched in Fig. 1.¹⁹ The hybridized states between CO and Pt are formed by the σ electron donation from the 5σ orbital of CO to the vacant $6sp$ conduction band of Pt and by the π electron back donation from $5d$ of Pt to the vacant $2\pi^*$ orbital of CO.^{20,21,23} The electron back donation into the $2\pi^*$ state of CO is mainly responsible for the weakening of the CO bond and hence the redshift of the CO stretch from 2170 cm^{-1} for free CO to 2090 cm^{-1} .²⁴ Participation of the 5σ orbital to the CO-Pt bond has been confirmed by ultraviolet photoemission spectroscopy that shows a significant shift of the photoemission peak of the 5σ orbital of CO upon adsorption on Pt.^{25,16}

For CO on the Pt(111) surface, the $5\sigma_b$ state shown in Fig. 1 has been measured by photoemission spectroscopy to be 9.6 eV below the Fermi energy E_F .^{25,16} The unoccupied $2\pi_a^*$ state has been identified to be 4.3 eV above E_F by inverse photoemission⁹ and two-photon photoemission.¹⁰ To the best of our knowledge, the energy level of the sp -derived state $5\sigma_a$ for CO on Pt(111) has never been detected, although the $5\sigma_a$ state for CO on Pt(110) has been suggested at 2 eV above E_F by inverse photoemission spectroscopy.²⁶ Our detection of the CO-related surface resonance allows us to determine the energy level of the $5\sigma_a$ state for atop CO on Pt(111). Studies by photoemission spectroscopy show that the density of states of the $5d$ band exhibits a broad distribution with two peaks at 0.3 and 4.3 eV below E_F ,²⁵ as shown in Fig. 1. The electronic transition from $5d$ at 4.3 eV below E_F to $5\sigma_a$ was beyond our probing range. The observed transition at 2.51 eV must arise from $2\pi_b^*$ at 0.3 eV below E_F to $5\sigma_a$. This then indicates that $5\sigma_a$ is 2.2 eV above E_F . As indicated by the arrow in Fig. 1, the $2\pi_b^*$ to the $5\sigma_a$ transition excites electrons into an antibonding orbital, and reduces the strength of CO-Pt bond. Theoretical calculations showed that the excitation may result in a repulsive potential between CO and Pt and lead to the desorption of ground-state CO molecules from the Pt surface.^{23,12} The d to s transition of pure Pt is optically forbidden, but the chemisorption of CO on Pt makes the transition allowed. Our measurements explain the observation that the threshold energy for neutral CO desorption from the Pt(111) surface lies above 2.3 eV.²²

It has been found that the sensitivity of SFG to CO at bridge sites of Pt(111) is much less than that to CO at atop sites, in contrast to IRAS.¹⁴ Our experimental results provide an explanation. The atop CO/Pt has an electronic resonance at 2.51 eV. Thus SFG detection of atop CO with a visible

input experiences a near-resonance enhancement. On the other hand, CO at bridge sites have a stretching mode that shows a larger redshift from that of free CO, indicating a weaker CO bond and a stronger interaction between CO and Pt. Theoretical calculation also suggests that the electronic excited state of a bridged CO/Pt has a higher energy than that of an atop CO/Pt.¹² Thus, with a visible input, SFG detection of the bridged CO/Pt is off-resonance and less sensitive. To enhance the SFG intensity of bridged CO, an UV input would be needed.

In summary, we have identified the lowest adsorbate-induced electronic state of atop CO on Pt(111) using two-dimensional IR-visible SFG spectroscopy. The observed

electronic resonance is at 2.51 eV with a bandwidth of 0.83 eV. The transition energy at 2.51 eV indicates that the $5\sigma_a$ antibonding state derived from mixing of Pt $6sp$ and CO 5σ for atop CO on Pt(111) is 2.2 eV above E_F . The measurements provide an experimental evidence for the contribution of chemical enhancement mechanism to surface-enhanced spectroscopy.

This work was supported by the Director, Office of Science, Office of Basic Energy Sciences, Division of Materials Sciences and Engineering, of the U.S. Department of Energy under Contract No. DE-AC03-76SF00098. S.W. is in part financed by Laboratory of Materials and Semiconductor Physics, Royal Institute of Technology, Sweden.

*Address after July 2004: Department of Chemistry, University of British Columbia, Vancouver, Canada.

[†]Electronic address: somorjai@socrates.berkeley.edu

¹Y.R. Shen, *Nature (London)* **337**, 519 (1989); Y. R. Shen, *Frontiers in Laser Spectroscopy*, edited by T. W. Hensch and M. Inguscio (North-Holland, Amsterdam, 1994), p. 139.

²Z. Chen, Y.R. Shen, and G.A. Somorjai, *Annu. Rev. Phys. Chem.* **53**, 437 (2002).

³M.B. Raschke, M. Hayashi, S.H. Lin, and Y.R. Shen, *Chem. Phys. Lett.* **359**, 367 (2002).

⁴*Frontier Orbitals and Reaction Paths*, edited by K. Fukui and H. Fujimoto (World Scientific, Singapore, 1997).

⁵*Surface Photochemistry*, edited by M. Anpo (Wiley, New York, 1996).

⁶M. Moskovits, *Rev. Mod. Phys.* **57**, 783 (1985).

⁷R. Leckey, *Ultraviolet Photoelectron Spectroscopy*, Vol. 22 (1992); M. H. Kibel, *X-ray Photoelectron Spectroscopy*, edited by von D. J. O'Connor, B. A. Sexton, and R. S. C. Smart, Springer Series in Surface Sciences, Vol. 23 (1992).

⁸N.M. Markovic and P.N. Ross, *Surf. Sci. Rep.* **45**, 121 (2002).

⁹V. Dose, J. Rogozik, A.M. Bradshaw, and K.C. Prince, *Surf. Sci.* **179**, 90 (1987).

¹⁰T. Anazawa, I. Kinoshita, and Y. Matsumoto, *J. Electron Spectrosc. Relat. Phenom.* **88-91**, 585 (1998)

¹¹J.I. Gersten, R.L. Birke, and J.R. Lombardi, *Phys. Rev. Lett.* **43**, 147 (1979).

¹²H. Nakatsuji, H. Morita, H. Nakai, Y. Murata, and K. Fukutani, *J. Chem. Phys.* **104**, 714 (1996).

¹³D. Y. Wu, X. Xu, Z. J. Cao, P. Shi, B. Ren, and Z. Q. Tian, *Proceedings of the Surface Raman Spectroscopy Symposium, Xiaman, China, 2000* (unpublished).

¹⁴C. Klunker, M. Balden, S. Lehwald, and W. Daum, *Surf. Sci.* **360**, 104 (1996)

¹⁵*CRC Handbook of Chemistry and Physics*, 83rd ed. (2003).

¹⁶D.A. Trenary, S.L. Tang, R.J. Simonson, and F.R. McFeely, *Surf. Sci.* **124**, 555 (1983)

¹⁷M. Hayashi, S.H. Lin, M.B. Raschke, and Y.R. Shen, *J. Phys. Chem. A* **106**, 2271 (2002).

¹⁸Y.J. Chabal, *Surf. Sci. Rep.* **8**, 211 (1988).

¹⁹G. Blyholder, *J. Phys. Chem.* **68**, 2772 (1964).

²⁰G.W. Smith and E.A. Carter, *J. Phys. Chem.* **95**, 2327 (1991).

²¹B. Hammer, Y. Morikawa, and J.K. Nørskov, *Phys. Rev. Lett.* **76**, 2141 (1996).

²²K. Fukutani, M. Song, and Y. Murata, *J. Chem. Phys.* **103**, 2221 (1995).

²³H. Aizawa and S. Tsuneyuki, *Surf. Sci.* **399**, L364 (1998).

²⁴F. Illas, S. Zurita, J. Rubio, and A.M. Márquez, *Phys. Rev. B* **52**, 12 372 (1995).

²⁵D.A. Shirley, J. Stohr, P.S. Wehner, R.S. Williams, and G. Apai, *Phys. Scr.* **16**, 398 (1977).

²⁶G. Rangelov, N. Memmel, E. Bertel, and V. Dose, *Surf. Sci.* **251**, 965 (1991).